PHYSICS AND CHEMISTRY OF SOLID STATE
V. 24, No. 3 (2023) pp. 578-583
Section: Chemistry

DOI: 10.15330/pcss.24.3.578-583

Vasyl Stefanyk Precarpathian National University

ФІЗИКА І ХІМІЯ ТВЕРДОГО ТІЛА
Т. 24, № 3 (2023) С. 578-583
Хімічні науки

UDC 546.682+548.734+669.18+544.653 ISSN 1729-4428

G. Nychyporuk[1], V. Kordan[1], M. Horiacha[1], B. Halyatovskii[1], O. Hudzo[1], V. Zaremba[1], V. Pavlyuk[1,2]

Crystal structure and electrochemical hydrogenation of $HoNiIn_{1-x}Al_x$ (x = 0-1) solid solution

[1]*Ivan Franko National University of Lviv, Lviv, Ukraine,*
[2]*Jan Długosz University of Czestochowa, Czestochowa, Poland, halyna.nychyporuk@lnu.edu.ua*

The influence of the substitution of indium by aluminum in HoNiIn compound at 873 K was investigated in the full concentration range by means of powder X-ray diffraction and EDX analysis. The formation of continuous solid solution was determined and changes of the unit cell parameters were calculated: $HoNiIn_{1.0-0}Al_{0-1.0}$ (ZrNiAl-type structure, space group P-62m, a = 0.74343(4)–0.69959(6) nm and c = 0.37472(3)–0.38289(4) nm, V = 0.17936(2)–0.16229(3) mn^3). The best discharge capacity after electrochemical hydrogenation studies of $HoNiIn_{1-x}Al_x$ solid solution is observed for battery prototypes with $HoNiIn_{0.2}Al_{0.8}$- and $HoNiIn_{0.4}Al_{0.6}$-based electrodes.

Keywords: powder data, solid solution, electrochemical hydrogenation.

Received 28 May 2023; Accepted 19 September 2023.

Introduction

Huge amount of ternary systems *R*-*T*-*X* (*R* – rare earth element, *T* - transition metal, *X* – p-element of III-IV groups) characterized by forming equiatomic compounds [1, 2] with magnetic and transport properties in a wide temperature range. HoNiIn compound has two successive magnetic phase transitions with increasing temperature [3]. Non-colinear antiferromagnetic HoNiIn with increasing indium content $HoNi_{1-x}In_{1+x}$ the values of the critical temperature of the magnetic ordering and paramagnetic Curie temperature decrease while the values of the effective magnetic moment do not change [4, 5]. The existence of two magnetic phases has been confirmed for HoNiAl compound by powder data [6].

The effect of the hydrogenation on the magnetic properties and crystal structure has been already studied for ternary aluminides *R*NiAl. For the majority of compounds hydrogenation leads to an orthorhombic distortion of the original hexagonal structure ZrNiAl [7-9]. The incorporation of hydrogen into HoNiAl compound leads to a decrease of the magnetic ordering temperature from 13 to 6 K. The crystal lattices of all compounds are anisotropically expanded. Moreover, the crystal symmetry is lowered to orthorhombic in $HoNiAlH_{2.0}$ [10].

The symmetry of the initial ZrNiAl-type structure is not changed by hydrogenation *R*NiIn compounds. Hydrogen insertion causes a pronounced anisotropic expansion of the unit cells. *R*NiIn compounds formed with Y or the heavier rare earth metals (*R* = Sm, Gd, Tb, Dy, Ho, Er and Tm) do not form hydrides at hydrogenation pressures up to 100 bar [11].

Here we report structure details and electrochemical hydrogenation data for the $HoNiIn_{1-x}Al_x$ solid solution phase.

I. Experimental details

Polycrystalline samples of $HoNiIn_{1-x}Al_x$ system (up to 1.0 g), with x range from 0 to 1.0 in steps of 0.1, were prepared by arc melting of the pure elements (all with stated purities better than 99.9%) under an argon atmosphere (purified using titanium sponge). The buttons were remelted twice to ensure homogeneity. Further all

samples were additionally sealed in evacuated silica ampules and then annealed for one month at 873 K, followed by quenching. The samples were analyzed by X-ray powder diffraction using a DRON 2.0M (Fe $K\alpha$-radiation) and STOE STADI P (Cu $K\alpha_1$-radiation) diffractometers. The phase analysis and structural calculations were based on the powder data using the program packages STOE WinXPOW [12] and FullProf [13].

The ability of the electrochemical hydrogenation was investigated in a two-electrode Swagelok-type cell. Hydrogensorption characteristics are measured over 50-charge-discharge cycles. Powdered alloys moistened with electrolyte (6M KOH solution) and compressed were used as anode. A mixture of freshly prepared, room-dried nickel(II) hydroxide and graphite (9:1 by weight) was used as cathodic material.

The morphology of the powder surface has been studied by scanning electron microscope Tescan Vega3 LMU. To determine the electrodes qualitative and quantitative composition, the methods of energy-dispersion X-ray (Oxford Instruments Aztec ONE analyzer) and X-ray fluorescent spectroscopy (ElvaX Pro spectrometer) were used. The integral composition for samples containing aluminum, was carried out in a pure helium medium, interpreting the "light" spectrum up to 8 keB.

II. Results and discussions

Substitution indium by aluminum leads to formation of continuous solid solution $HoNiIn_{1.0-0}Al_{0-1.0}$ with ZrNiAl-type structure according to the results of phase analysis. Except for the main phase, some samples additionally contain a small amount (up to 5%) of phase with $CaCu_5$-type structure. Results of EDX analysis of some samples are shown on Fig. 1. X-ray diffraction patterns and variation of the unit cell parameters within the solid solution $HoNiIn_{1-x}Al_x$ are shown on Fig. 2.

As HoNiIn and HoNiAl are isostructural compounds, the formatting of continuous solid solutions was expected. The refined parameter c of unite cell a bit increases with increasing aluminum content, while parameter a and cell volume V decrease. Such behavior of variation of the parameters for the solid solution was already observed in the similar systems $R NiIn_{1-x}Al_x$ with ZrNiAl- type structure [14-16].

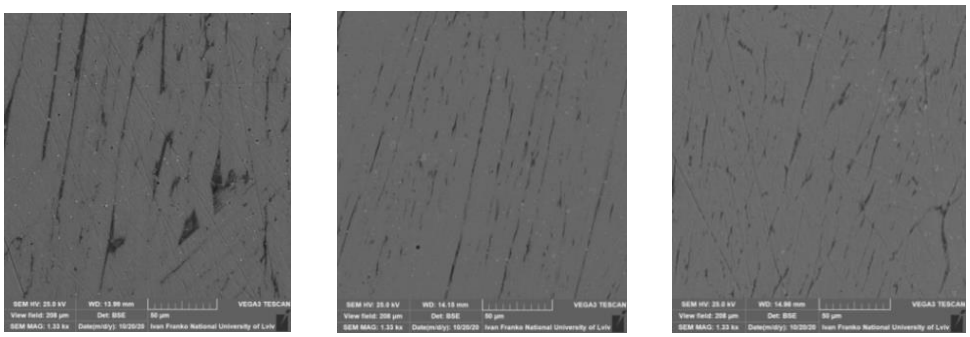

a *b* *c*

Fig. 1. Electron microphotographs of samples of the solid solution $HoNiIn_{1-x}Al_x$: (*a*) $HoNiIn_{0.7}Al_{0.3}$ (gray phase – $Ho_{0.34}Ni_{0.33}In_{0.26}Al_{0.07}$; dark phase – $Ho_{0.25}Ni_{0.48}In_{0.05}Al_{0.22}$), (*b*) $HoNiIn_{0.5}Al_{0.5}$ (gray phase – $Ho_{0.32}Ni_{0.33}In_{0.19}Al_{0.16}$; dark phase – $Ho_{0.24}Ni_{0.45}In_{0.05}Al_{0.26}$) and (*c*) $HoNiIn_{0.3}Al_{0.7}$ (gray phase – $Ho_{0.33}Ni_{0.33}In_{0.09}Al_{0.25}$; dark phase – $Ho_{0.21}Ni_{0.45}In_{0.04}Al_{0.30}$).

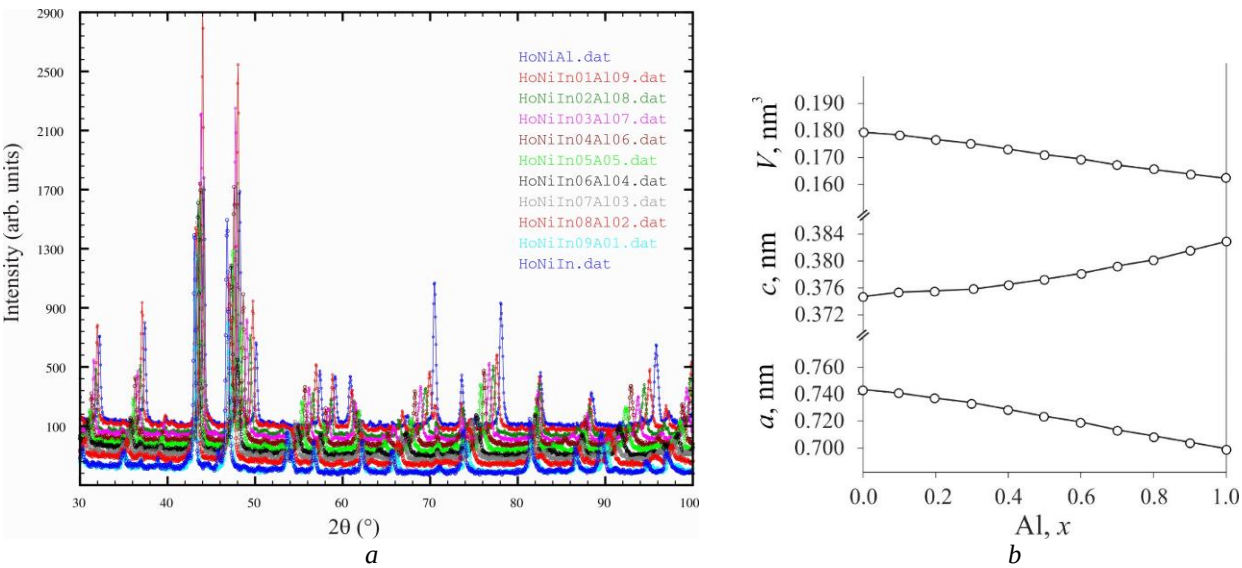

a *b*

Fig. 2. X-ray diffraction (DRON 2.0M, Fe $K\alpha$-radiation) patterns (*a*) and variation of the unit cell parameters (*b*) within the solid solution $HoNiIn_{1-x}Al_x$.

The refinement of crystal structure from powder diffraction data for the $HoNiIn_{0.6}Al_{0.4}$ sample confirms substituting indium by aluminum atoms in the crystallographic site 3*g* (ZrNiAl type structure, space group *P*-62*m*) (Fig. 3). The refined unit cell parameters for $HoNiIn_{0.6}Al_{0.4}$ are: a = 0.72835(5) nm, c = 0.37603(3) nm, V = 0.17276(2) nm^3, $B_{overall}$ = 0.58·10^2 nm^2; R_{Bragg} = 0.108, R_F = 0.089, and refined atomic coordinates: Ho (3*f*) 0.58699(3); 0; 0; Ni1 (2*d*) 1/3; 2/3; 1/2; Ni2 (1*a*) 0; 0; 0; *M* = 0.63(In) + 0.37(Al) (3*g*) 0.25279(5); 0; 1/2. Additionally, the sample contained phase $Ho(Ni,In,Al)_5$ ($CaCu_5$-type structure), the content of which did not exceed 2%.

We performed electrochemical hydrogenation for the few samples of the $HoNiIn_{1-x}Al_x$ solid solution with initial composition: x = 0; 0.2; 0.3; 0.4; 0.6; 0.7; 0.8 and 1. The electrochemical reactions that occur in the case of HoNiIn intermetallic as electrode can be presented by the following scheme:

$$HoNiIn + xH_2O + x\bar{e} \underset{\text{discharge (dehydrogenation)}}{\overset{\text{charge (hydrogenation)}}{\rightleftharpoons}} HoNiInH_x + xOH^-$$

$$Ni(OH)_2 + xOH^- \underset{\text{discharge (reduction)}}{\overset{\text{charge (oxidation)}}{\rightleftharpoons}} NiOOH + xH_2O + x\bar{e}$$

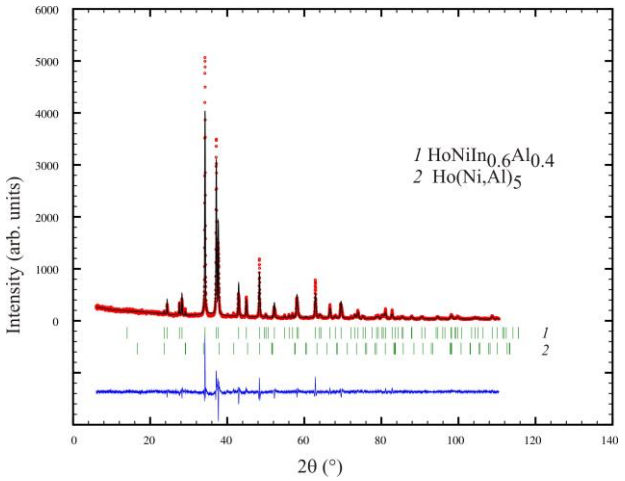

Fig. 3. Experimental (circles), calculated (continuous line) and difference (bottom) X-ray patterns of the $HoNiIn_{0.6}Al_{0.4}$ sample (STOE STADI P, Cu $K\alpha_1$-radiation).

X-ray powder patterns of $HoNiIn_{0.8}Al_{0.2}$ sample before and after hydrogenation are presented in Fig. 4. After hydrogenation we can see an amorphous halo at 20-35° 2θ and shifted the main diffraction peaks to the low angle area because of the formation of hydrides with bigger unit cell parameters. After hydrogenation, the unit cell parameters of hydrides have increased (Table 1). Hydrides can be presented as filled-up ZrNiAl-type.

X-ray fluorescence spectroscopy was used for study of the integral composition of electrode materials before and after hydrogenation. The ratio of Ho/Ni/*M* was close to equiatomic for all samples before hydrogenation and was approximately ~ 0.91/1.06/1.03 for most samples after hydrogenation. The morphology of the surface of studied samples is presented in Fig. 5. The shape of grains is block-like or irregular with etched edges. BSE-detector (right image, Fig. 5 *a*, *b*) showed the dark area for HoNiIn and $HoNiAl_{0.7}In_{0.3}$ samples after hydrogenation. These by-products phases are amorphous and represent the O-contained interphases.

Elemental mapping of electrode materials (powders) are presented in Fig. 6. It should be noted that some of the areas were etched by electrolyte solution and we can see dark areas (more content of O). In the cases of ternary alloy HoNiIn and tetrary $HoNiAl_{0.7}In_{0.3}$ we observed the decreasing of Ho-content due corrosion activity. In the case of ternary alloy HoNiAl the most loss of composition was for Al. We assumed the formation of amorphous $Al(OH)_3$ without high intensity diffraction peaks on the XRD powder patterns.

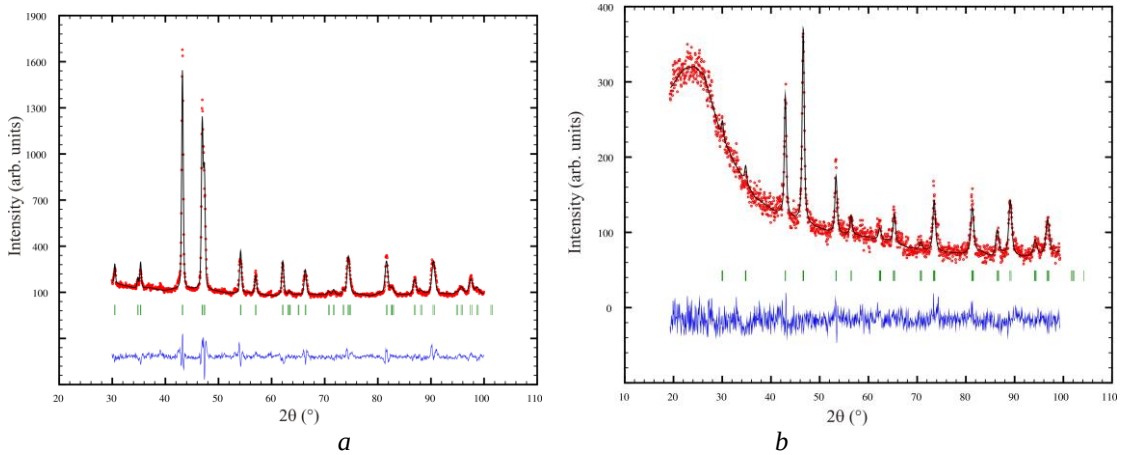

Fig. 4. Experimental (circles), calculated (continuous line) and difference (bottom) X-ray patterns of $HoNiIn_{0.8}Al_{0.2}$ sample before (*a*) and after (*b*) hydrogenation (DRON 2.0M, Fe $K\alpha$-radiation).

Table 1.

Unit cell parameters of selected phases in the $HoNiIn_{1.0–0}Al_{0–1.0}$ solid solution before (top) and after (bottom) hydrogenation

Composition	a, nm	c, nm	V, nm^3
$HoNiIn_{0.8}Al_{0.2}$	0.73701(8)	0.37558(5)	0.17668(3)
	0.74747(18)	0.37474(18)	0.18132(11)
$HoNiIn_{0.4}Al_{0.6}$	0.71940(4)	0.37816(3)	0.16949(2)
	0.74053(20)	0.37457(12)	0.17789(9)
$HoNiIn_{0.2}Al_{0.8}$	0.70907(6)	0.38017(4)	0.16554(2)
	0.73487(20)	0.37246(13)	0.17419(9)

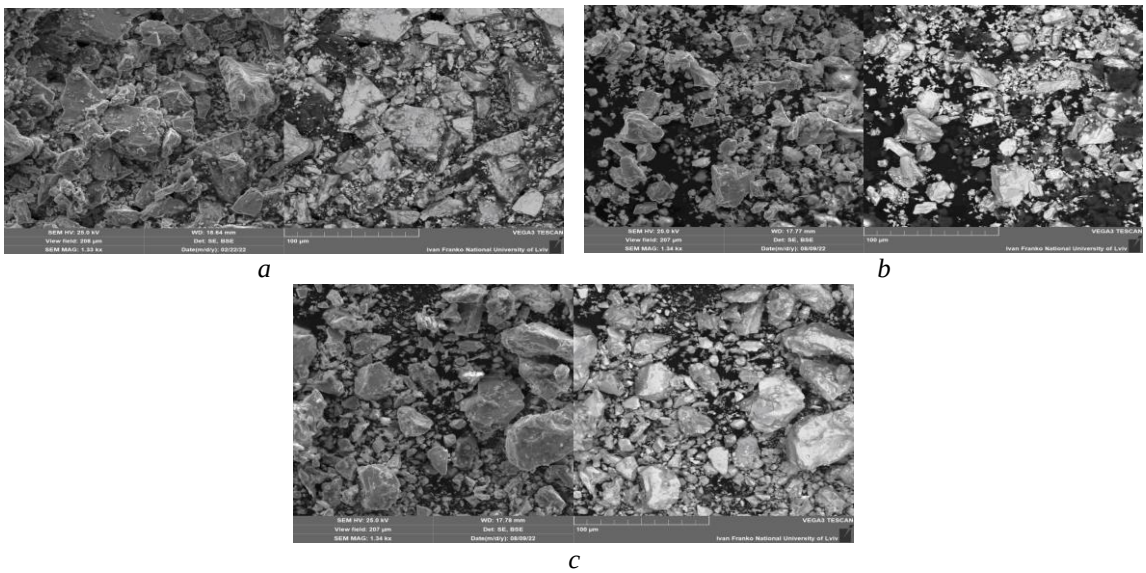

a *b* *c*

Fig. 5. SEM-images of HoNiIn (*a*), $HoNiAl_{0.7}In_{0.3}$ (*b*) and HoNiAl (*c*) after hydrogenation.

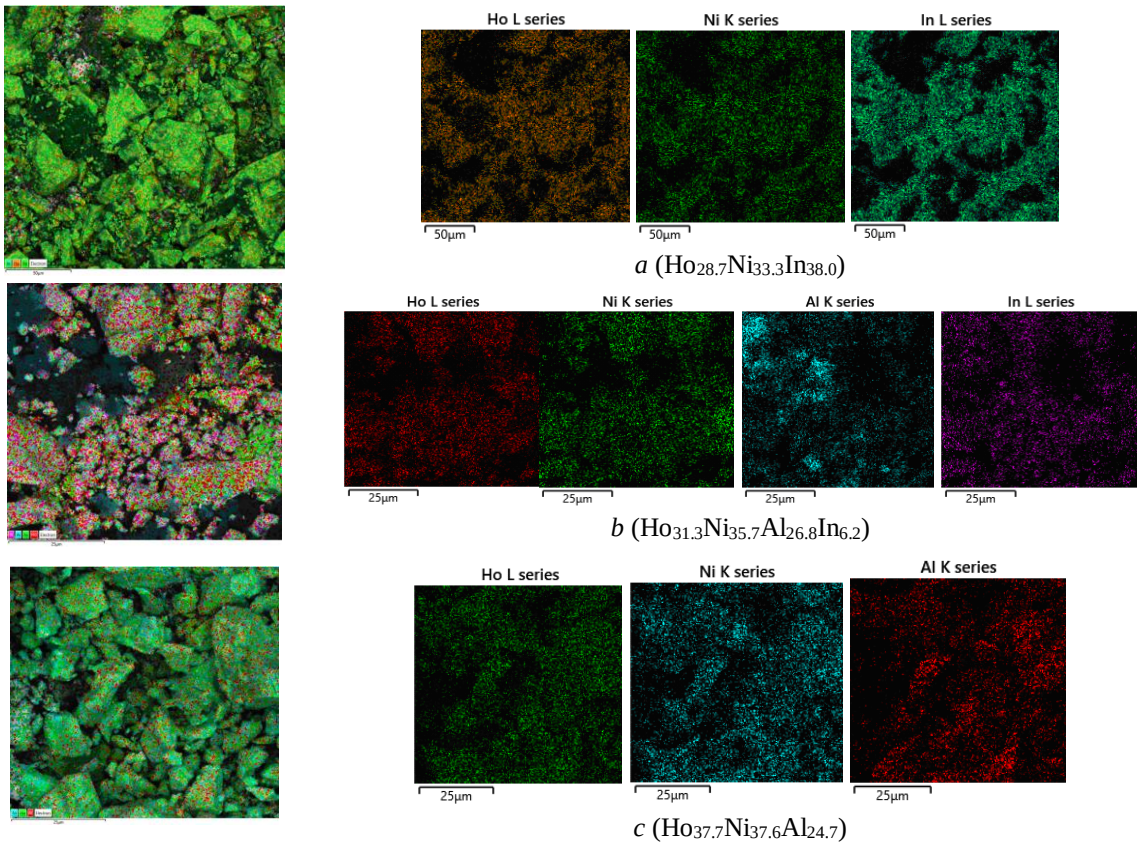

a ($Ho_{28.7}Ni_{33.3}In_{38.0}$)

b ($Ho_{31.3}Ni_{35.7}Al_{26.8}In_{6.2}$)

c ($Ho_{37.7}Ni_{37.6}Al_{24.7}$)

Fig. 6. Elemental mapping on the powder sample surfaces after electrochemical hydrogenation: HoNiIn (*a*), $HoNiAl_{0.7}In_{0.3}$ (*b*) and HoNiAl (*c*).

Selected charge and discharge curves for the battery prototypes with $HoNiIn_{1-x}Al_x$ alloy as a negative electrode are presented in Fig. 7. Different value of discharge capacity is easily explained by corrosion activity of alloys. Similar behavior was manifested in cases hydrogenation of solid solutions with $MgCu_2$ and $CaCu_5$-type structure [17-19].

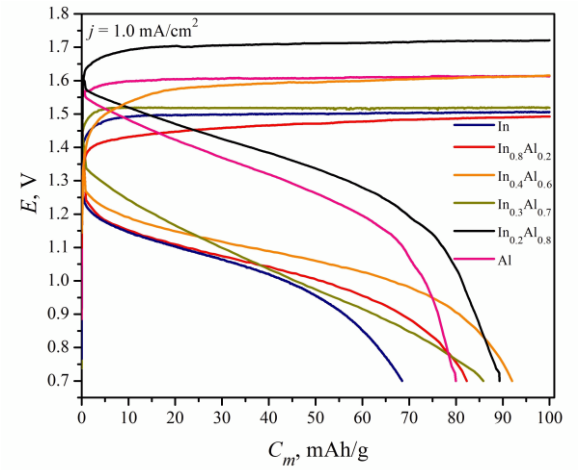

Fig. 7. Selected charge and discharge curves the battery prototypes with $HoNiIn_{1-x}Al_x$ alloy as electrode

Corrosion-resistant doping components in the electrode composition reduce the destruction of the material. Reducing of discharge capacity as a result of formation of the oxidation films on the grains and etching of surface and we observed for $La_2Mg_{17-x}M_x$ solid solution [20]. The biggest corrosion activity is observed for ternary HoNiIn, HoNiAl alloys and for tetrarny $HoNiIn_{0.8}Al_{0.2}$ sample. So, the surface of the electrode material is destroyed, the specific discharge capacity for these electrode materials is less. The best discharge capacity is observed for battery prototypes with $HoNiIn_{0.2}Al_{0.8}$- and $HoNiIn_{0.4}Al_{0.6}$-based electrodes (89.6 and 92.7 mAh/g, respectively). It should be noted that increasing an aluminum content causes the rise of nominal voltage.

Conclusions

Continuous solid solution forms in the $HoNiIn_{1-x}Al_x$ system. Substituting indium by aluminum atoms was confirmed by crystal structure refinement of $HoNiIn_{0.6}Al_{0.4}$ phase: a = 0.72835(5) nm, c = 0.37603(3) nm, V = 0.17276(2) nm^3, R_{Bragg} = 0.108, R_F = 0.089. Increasing an aluminum content causes the rise of nominal voltage. The highest nominal voltage was observed for $HoNiIn_{0.2}Al_{0.8}$ alloy.

Acknowledgment

This work was partly supported by the Simons Foundation (Award Number: 1037973).

Nychyporuk H. – Ph.D., Laboratory Chief Manager;
Kordan V. – Ph.D., Research Fellow;
Horiacha M. – Ph.D., Junior Research Fellow;
Halyatovskii B. – Student;
Hudzo O. – Student;
Zaremba V. – Ph.D., Associate Professor
Pavlyuk V. – DSc, Professor.

[1] Handbook of Inorganic Substances 2012 / Eds. P. Villars, K. Cenzual. (Berlin/Boston: De Gruyter GmbH & Co, 2012. 1574 p.)
[2] S. Gupta, K. G. Suresh, *Review on magnetic and related properties of RTX compounds*, J. Alloys Compd. 618, 562 (2015); https://doi.org/10.1016/j.jallcom.2014.08.079.
[3] H. Zhang, Z. Y. Xu, X. Q. Zheng, J. Shen, F. X. Hu, J. R. Sun, B. G. Shen, *Magnetocaloric effects in RNiIn (R = Gd-Er) intermetallic compounds*, J. Appl. Phys., 109, 123926-1 (2011); https://doi.org/10.1063/1.3603044.
[4] Y.B. Tyvanchuk, Y.M. Kalychak, Ł Gondek, M. Rams, A. Szytuła, Z. Tomkowicz, *Magnetic properties of $RNi_{1-x}In_{1+x}$ (R = Gd-Er) compounds*, J. Magn. Magn. Mater., 277, 368 (2004); https://doi.org/10.1016/j.jmmm.2003.11.018.
[5] Ł. Gondek, A. Szytuła, S. Baran, M. Rams, J. Hernandez-Velasco, Yu. Tyvanchuk, *Magnetic structures of non-stoichiometric hexagonal $RNi_{1-x}In_{1+x}$ (R = Dy, Ho, Er) compounds*, J. Magn. Magn. Mater., 278, 392 (2004); https://doi.org/10.1016/j.jmmm.2003.12.1324.
[6] N. K. Singh, K. G. Suresh, R. Nirmala, A. K. Nigam, S. K. Malik, *Effect of magnetic polarons on the magnetic, magnetocaloric, and magnetoresistance properties of the intermetallic compound HoNiAl*, J. Appl. Phys., 101, 093904-1 (2007); https://doi.org/10.1063/1.2724740.
[7] A.V. Kolomiets, L. Havela, V.A. Yartys, A.V. Andreev, *Hydrogen absorption-desorption, crystal structure and magnetism in RENiAl intermetallic compounds and their hydrides*, J. Alloys Compd., 253-254, 343 (1997); https://doi.org/10.1016/S0925-8388(97)02982-4.
[8] A.V. Kolomiets, L. Havela, A.V. Andreev, V. Sechovsky, V.A. Yartys, *RNiA1 hydrides and their magnetic properties*, J. Alloys Compd., 262-263, 206 (1997); https://doi.org/10.1016/S0925-8388(97)00382-4.
[9] H. W. Brinks, V. A. Yartys, B. C. Hauback, H. Fjellvåg, *Structure and magnetic properties of TbNiAl-based deuterides*, J. Alloys Compd., 330-332, 169 (2002);
[10] A. V. Kolomiets, L. Havela, D. Rafaja, H. N. Bordallo, H. Nakotte, V. A. Yartys, B. C. Hauback, H. Drulis, W. Iwasieczko, L. E. DeLong, *Magnetic properties and crystal structure of HoNiAl and UNiAl hydrides*, J. Appl. Phys., 87, 6815 (2000); https://doi.org/10.1063/1.372851.

[11] I. I. Bulyk, V. A. Yartys, R. V. Denys, Ya. M. Kalychak, I. R. Harris, *Hydrides of the RNiIn (R=La, Ce, Nd) intermetallic compounds: crystallographic characterisation and thermal stability*, J. Alloys Compd., 284, 256 (1999); https://doi.org/10.1016/S0925-8388(98)00953-0,

[12] STOE WinXPOW, Version 1.2, STOE & CIE GmbH. Darmstadt, 2001.

[13] J. Rodríguez-Carvajal, *Recent Developments of the Program FULLPROF*, Commission on Powder Diffraction (IUCr). Newsletter, 26, 12 (2001).

[14] M. Horiacha, L. Zinko, G. Nychyporuk, R. Serkiz, V. Zaremba, *The $GdTIn_{1-x}M_x$ (T = Ni, Cu; M = Al, Ga; 0 < x < 1) systems*, Visnyk Lviv Univ. Ser. Chem., 58, 77 (2017). [in Ukrainian]

[15] M. Horiacha, I. Savchuk, G. Nychyporuk, R. Serkiz, V. Zaremba, *$YNiIn_{1-x}M_x$ (M = Al, Ga, Sb) systems*, Visnyk Lviv Univ. Ser. Chem., 59, 67 (2018). [in Ukrainian]

[16] M. Horiacha, B. Halyatovskii, S. Horiacha, G. Nychyporuk, R. Pöttgen, V. Zaremba, *The $TbNiIn_{1-x}M_x$ (M = Al, Ge, Sb) systems*, Visnyk Lviv Univ. Ser. Chem., 61, 52 (2020); [in Ukrainian] https://doi.org/10.30970/vch.6101.052.

[17] N. O. Chorna, V. M. Kordan, A. M. Mykhailevych, O. Ya. Zelinska, A. V. Zelinskiy, K. Kluziak, R. Ya. Serkiz, V. V. Pavlyuk, *Electrochemical hydrogenation, lithiation and sodiation of the $GdFe_{2-x}M_x$ and $GdMn_{2-x}M_x$ intermetallics*, Voprosy khimii i khimicheskoi tekhnologii, 2, 139 (2021); https://doi.org/10.32434/0321-4095-2021-135-2-139-149.

[18] I. Stetskiv, V. Kordan, I. Tarasiuk, V. Pavlyuk, *Synthesis, crystal structure and physical properties of the $TbCo_{4.5}Si_xLi_{0.5-x}$ solid solution*, Physics and Chemistry of Solid State, 22(3), 577 (2021); https://doi.org/10.15330/pcss.22.3.577-584.

[19] B. Rożdżyńska-Kiełbik, I. Stetskiv, V. Pavlyuk, A. Stetskiv, *Significant improvement of electrochemical hydrogenation, corrosion protection and thermal stability of $LaNi_{4.6}Zn_{0.4-x}Li_x$ ($x \leq 0.2$) solid solution phases due to Li-doping*, Solid State Sci. 113, 106552 (2021); https://doi.org/10.1016/j.solidstatesciences.2021.106552.

[20] V. Kordan, V. Nytka, I. Tarasiuk, O. Zelinska, V. Pavlyuk, *Synthesis, crystal structure, and electrochemical hydrogenation of the $La_2Mg_{17-x}M_x$ (M = Ni, Sn, Sb) solid solutions*, Eur. J. Chem. 12(2), 197 (2021); https://doi.org/10.5155/eurjchem.12.2.197-203.2092.

Г. Ничипорук[1], В. Кордан[1], М. Горяча[1], Б. Галятовський[1], О. Гудзьо[1], В. Заремба[1], В. Павлюк[1,2]

Кристалічна структура і електрохімічне гідрування твердого розчину $HoNiIn_{1-x}Al_x$ (x = 0-1)

[1]*Львівський національний університет імені Івана Франка, Львів, Україна,*
[2]*Гуманітарно-природничий університет імені Яна Длугоша, Ченстохова, Польща,* halyna.nychyporuk@lnu.edu.ua

Вплив заміщення індію на алюміній у сполуці HoNiIn досліджено методами рентгенівської дифракції і EDX аналізу у повному концентраційному інтервалі за температури 873 K. Визначено утворення і уточнено параметри елементарної комірки неперервного твердого розчину $HoNiIn_{1,0-0}Al_{0-1,0}$ (структурний тип ZrNiAl; просторова група P-62m; a = 0,74343(4)–0,69959(6); c = 0,37472(3)–0,38289(4) нм, V = 0,17936(2)–0,16229(3) нм^3).

Найкраща розрядна здатність після досліджень електрохімічного гідрування твердого розчину $HoNiIn_{1,0-0}Al_{0-1,0}$ спостерігається для прототипів акумуляторів з електродами на основі фаз $HoNiIn_{0,2}Al_{0,8}$ та $HoNiIn_{0,4}Al_{0,6}$.

Ключові слова: метод порошку, твердий розчин, електрохімічне гідрування.